AUTHOR QUERY FORM

ELSEVIER

Journal: POWER

Article Number: 18548

Please e-mail or fax your responses and any corrections to:

E-mail: corrections.eseo@elsevier.tnq.co.in

Fax: +31 2048 52789

Dear Author,

Please check your proof carefully and mark all corrections at the appropriate place in the proof (e.g., by using on-screen annotation in the PDF file) or compile them in a separate list. Note: if you opt to annotate the file with software other than Adobe Reader then please also highlight the appropriate place in the PDF file. To ensure fast publication of your paper please return your corrections within 48 hours.

For correction or revision of any artwork, please consult http://www.elsevier.com/artworkinstructions.

Any queries or remarks that have arisen during the processing of your manuscript are listed below and highlighted by flags in the proof.

Location in article	Query / Remark: Click on the Q link to find the query's location in text Please insert your reply or correction at the corresponding line in the proof
Q1	Please check whether the designated corresponding author is correct, and amend if necessary.
Q2	Fig. 11 was not cited in the text. Please check that the citations suggested by the copyeditor is in the appropriate place, and correct if necessary.
Q3	Please confirm that given names and surnames have been identified correctly.
	Please check this box or indicate your approval if you have no corrections to make to the PDF file ☐

Thank you for your assistance.

Journal of Power Sources xxx (2014) 1–8

Contents lists available at ScienceDirect

Journal of Power Sources

journal homepage: www.elsevier.com/locate/jpowsour

A practical framework of electrical based online state-of-charge estimation of lithium ion batteries

Feng Leng [a,b,*], Cher Ming Tan [a,b], Rachid Yazami [a,b], Minh Duc Le [a]

[a] Nanyang Technological University, School of Electrical Electronics Engineering, Blk S2.1, 50 Nanyang Avenue, Singapore 639798, Singapore
[b] TUM CREATE, 1 Create Way, #10-02 Create Tower, Singapore 138602, Singapore

HIGHLIGHTS

- We develop an electrical model based on the principle of electrochemistry.
- This model agrees well with its experimental EIS spectra and discharging curve.
- The maximum initial capacity can be obtained simply through its discharging curve.
- Enable on-line estimation of the capacity used to indicate the SoC.

ARTICLE INFO

Article history:
Received 20 November 2013
Received in revised form
2 January 2014
Accepted 3 January 2014
Available online xxx

Keywords:
State of charge
Electrical model
Rest time
Electrochemical impedance spectroscopy
Warburg element
Butler–Volmer

ABSTRACT

State of charge (SoC) is an important parameter for li ion battery (LiB) cells, and its estimation should be done online as its continuous operation before recharge depends on its SoC. While Coulomb counting method (also called Coulometry) is useful to estimate the SoC online, its accuracy depends on the value of its initial maximum capacity. Presently, this capacity is obtained by the periodic discharge of the cell fully but this can introduce damage to the cell and shorten its lifespan. In this work, an electrical model is developed for LiB cells based on the principle of electrochemistry from its discharge curve (i.e. the change in terminal voltage over time within a discharge cycle). This model is able to compute the internal parameters of a cell, including its maximum initial capacity at the beginning of each discharge cycle. With the internal parameters computed, it can also produce its Nyquist plot and the plot is found to agree well with its experimental electrochemical impedance spectroscopy (EIS) spectra. With this model, the status of a LiB cell and its maximum charge capacity can be determined in real time.

1. Introduction

Batteries are playing an increasingly significant role in our daily life as electronic technology is occupying in more aspects of our lives such as portable communication devices including smart phones and laptops etc, portable medical information devices, and now electrification transportation systems. For light weight and long life applications, and clean environmental consideration, LiB stand up among various existing rechargeable batteries, due to its largest energy-to-weight ratio and long life as well as its memory-less property. Hence, it is a prime candidate for the portable devices' battery as well as electrical vehicles (EVs) of different kinds [1].

In all battery operated devices and system that require continuous operations, estimation of the battery SoC is important so that user can have a clue on the remaining useable time they can use further. Uncertainties in SoC estimation can cause the user to be highly conservative, but frequent re-charging can shorten the life-span of the battery [2]. On the other hand, if re-charging is done too late, an over-discharge may occur which also shorten the life of the battery.

Methods of SoC estimation can be classified into electrical, stochastic and thermodynamic methods [3]. In electrical methods, the commonly employed methods today are the Coulomb counting and open circuit voltage (OCV) methods. The Coulomb counting method integrates the current over time and thus the accumulated charge delivered can be obtained and used to estimate the SoC [4]. This method is simple and easy to be implemented, but its drawback is that its maximum capacity at the start of each discharge cycle must be known and this capacity degrades with prolonged charge–discharge cycle. Thus, this method often requires periodic

* Corresponding author. Nanyang Technological University, School of Electrical Electronics Engineering, Blk S2.1, 50 Nanyang Avenue, Singapore 639798, Singapore.
E-mail address: fleng001@e.ntu.edu.sg (F. Leng).

0378-7753/$ – see front matter © 2014 Published by Elsevier B.V.
http://dx.doi.org/10.1016/j.jpowsour.2014.01.020

capacity calibration where a full discharge of the cell will be performed, but such action can shorten the life of the battery significantly [5]. Another common method on the estimation of SoC is the OCV method [6], this method is not an online estimation as OCV can only be measured at open circuit. Also, OCV vs. SoC profiles can be very flat, and thus large uncertainty can be generated by using OCV to estimate SoC.

As errors can occur during the SoC measurement due to noise and external disturbance, Kalman filter (KF) has also been applied to estimate the battery's SoC as a stochastic method. It has become popular due to its self-regulated and online nature. As the SoC pattern with discharging is not linear, extended Kalman filter (EKF) and sigma-point Kalman filter (SPKF) are introduced, and they have been used for the lithium polymeric battery (LiPB)-based hybrid electric vehicle (HEV) battery [7–11]. As all the stochastic methods require an accurate model of the battery's discharging behaviour, various battery models [12] have been developed based on the battery electrical performances at the beginning, and these models are empirical instead of being derived based on the principle of electrochemistry, rendering their limited applicability to specific battery type without performance ageing being taken into account. Although there is a fully described model which takes into account of all the electro-chemical processes [13], it is very difficult to implement in real time application as complex solution of simultaneous partial differential equations is needed.

Thermodynamics based method computes the entropy of a cell based on the variation of the terminal voltage and temperature, from which the cell's SoC can be deduced [14]. Unfortunately its in-situ online measurement is yet to be developed.

Among all the online SoC measurement methods, Coulomb counting method is the most intuitive and simple. In order to remove the necessity of calibration to determine its maximum capacity at the start of each discharge cycle, an in-situ method is proposed to provide an accurate online estimation of the maximum capacity in this work.

As only the battery discharge curve is available during battery operation, the estimation will be done by extracting the information contained in the discharge curve. Thus decomposition of the curve into different components is necessary and it is the first step in the model development.

2. Decomposition of battery discharge curve

The discharging terminal voltage contains much information about the battery's working state. It is well understood that the terminal voltage can be decomposed into the electromotive force (emf) and the over-potential.

2.1. Derivation of emf expression

The emf represents the battery's ability to provide a certain voltage. It is the difference in equivalent potentials between the two electrodes. The emf is often measured as the OCV of the battery and is described by the Nernst's equation [13].

To model the emf voltage change during discharging, Coleman et al. [4] presented a linear relationship between the emf voltage and SoC based on their experimental data, but such linear relationship is applicable to a limited range of SoC, and it is empirical with the data set they have.

In fact, during discharging, the active mass concentrations at the electrodes reduces, render the reduction in its emf, and such active mass concentration reduction need to be taken into account to reflect the mechanism underlying.

Limit the work to the LiB of intercalation type reaction instead of displacement or conversion type reaction, the emf expression derived by Pop et al. [15] is employed, based on the Nernst Equation as given below:

$$V_{\mathrm{emf}} = E^{+}_{\mathrm{eq}} - E^{-}_{\mathrm{eq}} \tag{1}$$

where

$$E^{+}_{\mathrm{eq}} = E^{+}_{0} - \frac{RT}{F}\left[\ln\left(\frac{x_{\mathrm{Li}}}{1-x_{\mathrm{Li}}}\right) + U^{+}_{\mathrm{j}}x_{\mathrm{Li}} - \zeta^{+}_{\mathrm{j}}\right] \tag{2}$$

$$E^{-}_{\mathrm{eq}} = E^{-}_{0} - \frac{RT}{F}\left[\ln\left(\frac{z_{\mathrm{Li}}}{1-z_{\mathrm{Li}}}\right) + U^{-}_{\mathrm{j}}z_{\mathrm{Li}} - \zeta^{-}_{\mathrm{j}}\right] \tag{3}$$

Here R is the gas constant, F is the Faraday constant, T is temperature at the electrode in K, x_{Li} and z_{Li} are the mole fraction of $Li+$ ion inside the positive and negative electrodes respectively. U^{+}_{j} and U^{-}_{j} are the dimensionless interaction energy coefficient in the respective electrodes, and ζ^{+}_{j} and ζ^{-}_{j} are dimensional constant accounting for the phase transition in the equilibrium potential of the two electrodes. Superscripts + and − refer to positive and negative electrodes respectively. Subscript j is used to represent the phase change at the electrodes, and such phase change is found to occur at SoC below 50% (i.e. x_{Li} below 0.75 and z_{Li} below 0.25) [15]. As the terminal voltage of LiB will drop abruptly when SoC is below 50% for the ageing battery [2], the situation of SoC >50% is considered for practical consideration and hence the subscripts in Eqs. (1)–(3) are dropped in the subsequent equations.

If Q_{m} is the maximum amount of electrochemically active $Li+$ ion inside a battery, and the maximum capacities of the positive and negative electrodes are denoted as Q^{+}_{max} and Q^{-}_{max} , then according to the work of Pop et al. [15].

$$Q^{+}_{\mathrm{max}} = m_1 Q_{\mathrm{m}},\ m_1 \le 1 \tag{4}$$

$$Q^{-}_{\mathrm{max}} = m_2 Q_{\mathrm{m}},\ m_2 \le \frac{1}{2} \tag{5}$$

Here $m_1 = 1$ and $m_2 = 2$ for fresh battery, and corresponds to the chemical reaction of the full cell as schematized below:

$$C_6 + 2\mathrm{Li(NMC)O_2} \rightleftarrows \mathrm{LiC_6} + 2\mathrm{Li_{0.5}(NMC)O_2} \tag{6}$$

In Eq. (6) C_6 and $\mathrm{Li(NMC)O_2}$ denote the composition of the anode and the cathode at the cell discharge state respectively, whereas $\mathrm{LiC_6}$ and$\mathrm{Li_{0.5}(NMC)O_2}$ refer to the same electrodes composition at the cell' charge state.

Denote Q^{-}_{0} as the amount of Li+ ions inside the negative electrode in a fully discharged battery, and Q^{-}_{z} as the charge stored in the negative electrode for a given SoC, and consider the minimum SoC for practical application to be above 50% (in order to prevent over-discharge so as to maintain the battery lifespan), equation in Ref. [15] becomes

$$Q^{-}_{z} = Q^{-}_{0} + \mathrm{SoC} \times \left(Q_{\mathrm{m}} - Q^{-}_{0} - \frac{Q^{+}_{\mathrm{max}}}{2}\right) = \mathrm{SoC} \times Q_{\mathrm{m}}\left(1 - \frac{m_1}{2}\right) \tag{7}$$

since $Q^{-}_{0} \ll Q_{\mathrm{m}}$ and for SoC > 50%.

But z_{Li} and x_{Li} are given as [15],

$$z_{\mathrm{Li}} = \frac{Q^{-}_{z}}{Q^{-}_{\mathrm{max}}} \tag{8}$$

$$x_{\mathrm{Li}} = \frac{Q_{\mathrm{m}} - Q^{-}_{z}}{Q^{+}_{\mathrm{max}}} \tag{9}$$

Hence

$$z_{\mathrm{Li}} = SoC\frac{2-m_1}{2m_2} \tag{10}$$

$$x_{\mathrm{Li}} = \frac{Q_{\mathrm{m}}\left[1-\mathrm{SoC}\times\frac{2-m_1}{2}\right]}{m_1 Q_{\mathrm{m}}} = \frac{2-\mathrm{SoC}(2-m_1)}{2m_1} \tag{11}$$

and

$$V_{\mathrm{emf}} = E_{\mathrm{eq}}^{+} - E_{\mathrm{eq}}^{-}$$

$$= E_0 - \frac{RT}{F}\left\{\ln\frac{[2-(2-m_1)\mathrm{SoC}][2m_2-(2-m_1)\mathrm{SoC}]}{[2m_1-2+(2-m_1)\mathrm{SoC}][(2-m_1)\mathrm{SoC}]} + \left[\frac{U^{+}}{m_1}-\frac{2-m_1}{2m_1m_2}\times\mathrm{SoC}\times\left(m_2U^{+}-m_1U^{-}\right)\right]+\varepsilon\right\} \tag{12}$$

where $\varepsilon = \zeta^{+}-\zeta^{-}$, and $\mathrm{SoC} = Q_{\mathrm{m}} - \int i\mathrm{d}t/Q_{\mathrm{m}}$

2.2. Over-potential

The discharge over-potential results from the voltage drop due to electrodes potential and the internal impedances of a cell. Currently, there are three types of over-potential models available for LiB, namely the electrochemical, mathematical and electrical models [16]. Electrochemical models typically are computationally time consuming and are thus not suitable for online estimation. Mathematical models use stochastic approaches or empirical equations, and have no direct relation between the model parameters and the electrical characteristics of the batteries. Electrical models are the most intuitive for use in circuit simulations and online estimation of battery states. Within the electrical modes there are three different categories, namely the Thevenin-based, impedance-based and runtime-based models.

Thevenin-based model assumes the OCV is constant, but the emf or OCV is decreasing due to the decrease in SoC as mentioned earlier, it cannot represent the actual battery operation. Impedance-based models are usually obtained from fitting complicated equivalent networks to their EIS spectrum and are thus work only for fixed SoC and temperature setting [17], and

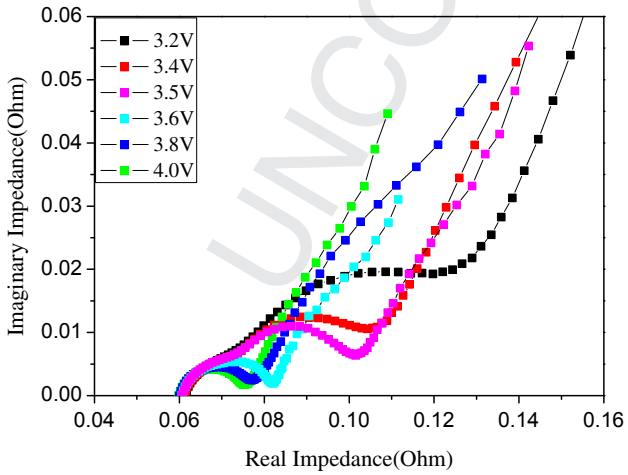

Fig. 1. EIS spectrum of Panasonic's CGR18650CH LiB cell at various OCV under Lab's ambient temperature of 23 °C. The solid line in different colour represents the impedance at various OCV (with corresponding SoCs).

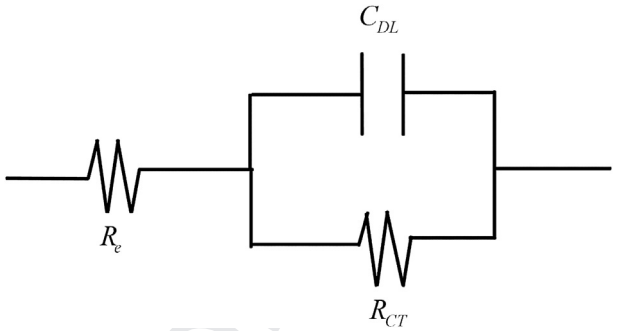

Fig. 2. Simple Randles' model for electrochemical cell.

cannot be used to predict battery runtime. Runtime-based model assumes a constant discharge current, and is not suitable for practical electric vehicle applications. Chen et al. [17] attempted to combine the three electrical models, but the relationship of OCV with SoC is obtained through curve fitting. In fact, almost all the equivalent circuits are derived from the measurement data without consideration of the mechanisms occurring in the battery during discharging.

From the typical EIS spectrum of LiB as shown in Fig. 1 and the electrochemical dynamics of charge transfer and diffusion in the battery, the simple Randle's model can be expanded as shown in Fig. 2 to construct an equivalent circuit of a battery based on the understanding of the mechanisms within the battery during discharging.

Solartron model 1400A with a Frequency Response Analyser (FRA) and an electrochemical interface (ECI) are used for our EIS measurement shown in Fig. 1. The battery cell is initially charged or discharged to the pre-set terminal voltage, and it is then withdrawn from the DC supply and rest for 2 h in order to attain a stable terminal voltage. An AC voltage of 5 mV over a span of frequencies from 0.001 Hz to 100 KHz is then applied to the cell without any DC current through the cell. In the simple Randles' model [18] shown in Fig. 2, the series resistance represents the ohmic resistance of the electrolyte and the electrodes, the RC circuit represents the charge transfer resistance R_{CT} and the double layer capacitor C_{DL}. One should also add the Warburg element as the mass transport of active mass is mostly diffusion limited [19], and the Warburg element in this proposed model belongs to the case of semi-infinite diffusion layer as revealed from experimental EIS spectrum of the LiB studied, Thus the corresponding impedance of Warburg element is given by Ref. [19]

$$Z_{\mathrm{w}} = \frac{\sigma}{\sqrt{\omega}} - j\frac{\sigma}{\sqrt{\omega}} \tag{13}$$

With the consideration of this mixed kinetic and charge transfer control, an equivalent circuit is constructed as in Fig. 3 [12,20]. Here

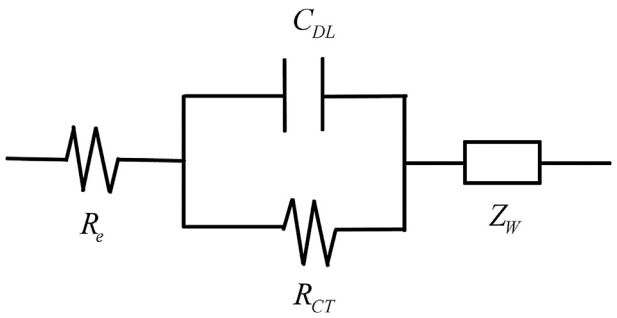

Fig. 3. Equivalent circuit with mixed kinetic and charge transfer control.

the Warburg element is placed outside the C_{DL} because the element describes the diffusion of the ions in electrolyte while C_{DL} and R_{CT} are modelling the process at the electrodes.

In a continuous discharging operation of battery, reduction in the active mass concentration at the porous electrode will occur. This reduction will change the emf due to the Nernst Equation which can only be applied for zero current, and this has been accounted for it in the previous section. This is a thermodynamics effect. The reduction in the active mass concentration also affects the kinetics of electrochemical reactions at the electrodes, and thus affects the over-potential [21]. Such effect can be taken into account by including the Butler–Volmer term in our model, and the corresponding impedance presented by this term is given by Ref. [22]

$$Z_{BV} = k\frac{Q_m}{Q_m - \int idt} \tag{14}$$

where the symbols have the same meaning as in Eq. (1), and k is called the rate of constant for electrode reaction.

Since the Butler–Volmer term accounts for the process at the electrodes, Z_{BV} should be in series with R_{CT}, and therefore the equivalent circuit model for a LiB cell is as shown in Fig. 4.

2.3. Temporal model of discharge curve

Based upon the understanding of the mass transport and electrochemical kinetics in the cell, and together with the EIS spectrum, an equivalent circuit of a cell as shown in Fig. 4 can be constructed. This equivalent circuit is however a frequency approach. In actual online application, only the electrical characteristics in time domain is available, and temporal approach must be adopted if SoC information is to be extracted online from the discharge curve of a battery cell [12].

For temporal approach, the Warburg element is to be represented using RC circuit. Through the inverse Laplace transform of the Warburg impedance, it is found that the temporal expression of the Warburg impedance is as follows [23]:

$$Z_\omega = \sum_{n=1}^{\infty} \frac{1}{C_\omega} \exp\frac{-t}{R_n C_\omega} \tag{15}$$

and

$$R_n = \frac{8k_1}{(2n-1)^2\pi^2} \tag{16}$$

$$C_\omega = \frac{k_1}{2k_2^2} \tag{17}$$

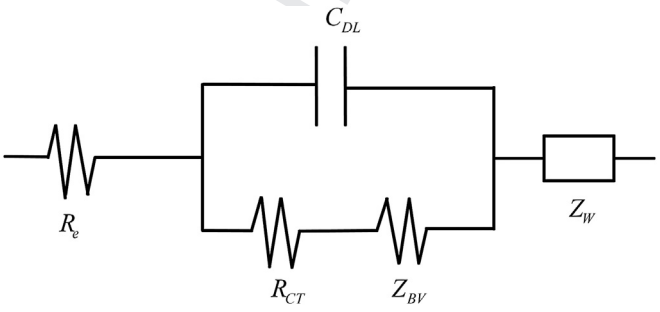

Fig. 4. Equivalent circuit model based on EIS spectrum.

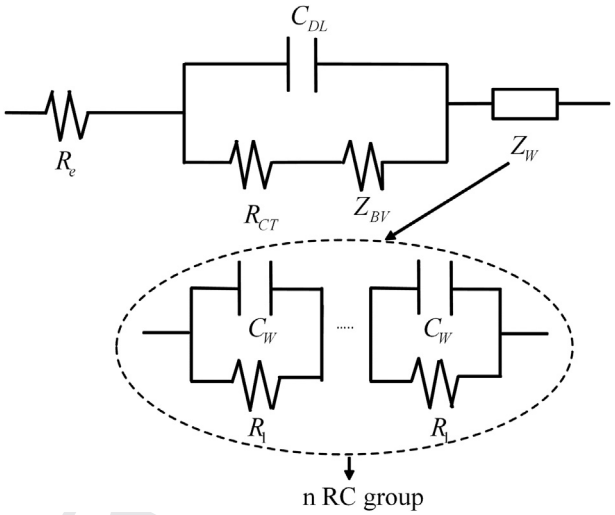

Fig. 5. Temporal equivalent circuit of LiB cell in this work.

Thus, the temporal equivalent circuit of the LiB cell can be represented in Fig. 5:

The equivalent circuit shown in Fig. 5 is however too complex for obtaining time domain relationship between the terminal voltage and discharging current of the cell. On the other hand, since the time constant due to C_{DL} (in the order of 10^{-3} ms to 10 s) is much smaller than that due to the Warburg element and the Butler–Volmer term (in the order of 1 s to 10^4 h) as shown by Jossen [19], and the goal here is to obtain the value of Q_m, the initial exponential decay (just 0.03 s) of the discharging curve can be ignored, and the following circuit (without C_{DL}) is thus used to fit the latter part of the discharging curve and obtain the parameters values of the circuit elements using a non-linear regression method, Levenberg–Marquart fitting Algorithm (LMA) cum Simulated Annealing (SA). SA [24] is employed to approximate global minima, and LMA is used to delivers rapid and accurate estimates of the global minima due to gradient-descent based algorithm [25]. With these algorithms, the fitting can agree well with the experimental results in around 0.3 s computed by i7 8-core CPU.

Theoretically, n should be infinity in order to have the RC circuit to represent the Warburg element. Practically, the value of n should be determined such that so long as the estimated values of the parameters in the equivalent circuit shown in Fig. 6 converge. Thus, SA cum LMA are applied to fit the circuit of Fig. 6 and the actual discharging curve with different values of n so as to determine the required number of n and at the same time, to obtain the parameters values.

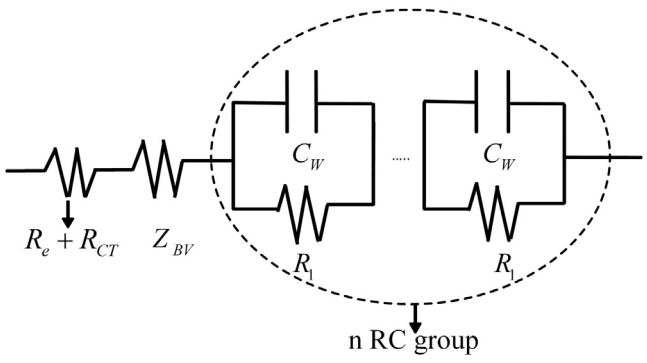

Fig. 6. Modified temporal equivalent circuit.

Table 1
CGR18650CH LiB specification [26].

Battery	Characteristics
Series	Panasonic Solid Solution (PPS)
Chemical system	$LiNiMnCoO_2$ (NMC)
Nominal voltage	3.6 V
Capacity	2,250 mAh Typical
Charging condition	CVCC 4.2 V max.0.7 C-rate (1500 mA), 110 mA cut-off 25 °C
Discharging condition	Constant current, 3.0 V cut-off 25 °C
Max discharge current	10 A (25° C)
Diameter (with tube)/Max.	18.6 (mm)
Height (with tube)/Max	65.2 (mm)
Approx. weight	44 (g)

With the equivalent circuit and the emf expression, the terminal voltage of a LiB cell can now be written as follows:

$$V_{\text{terminal}} = V_{\text{emf}} - \eta \tag{18}$$

where V_{emf} is given by Eq. (12), and the over-potential η is given below, based on the equivalent circuit in Fig. 6.

$$\eta(t) = i(t)\left(R_e + R_{CT} + k\frac{Q_m}{Q_m - \int_0^t i(\tau)\mathrm{d}\tau} + \sum_{n=1}^{\infty}\left(1-\exp\left(-\frac{t}{R_n C_w}\right)\right)R_n\right) \tag{19}$$

As this is a first attempt to relate the electrochemical processes in LiB to the components in electrical equivalent circuit, this work is limited to the following situation:

- The self-discharge behaviour of the battery is not considered. This can be considered only if the electrochemistry process of the self-discharging is well understood.

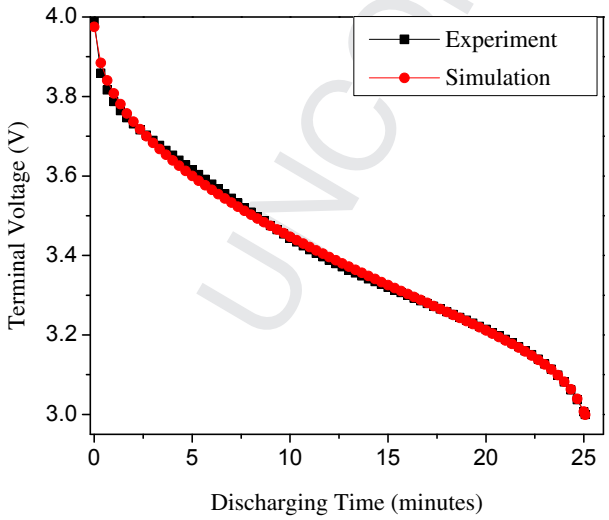

Fig. 7. Comparison of Experimental and computed discharge curve of Panasonic's CGR18650CH LiB cell. Discharge curve of tested cell at 2C under Lab's ambient temperature of 23 °C until the terminal voltage drop to cut-off voltage of 3 V.

- The temperature of the battery during discharging is assumed to be constant. This will be considered in future work with experimental data. The model in this work can easily be extended to include the temperature effect by making the components in the equivalent circuit to be temperature dependent.
- SoC is always above 50% for practical consideration. Extension to SoC all the way to 20% will be considered in future.
- No high discharging current (i.e. <10A) so that Peukert effect is insignificant.

3. Experimentation and analysis

In order to obtain the discharging curves of LiB, the following experiments are performed. Panasonic's CGR18650CH LiB is selected for all the experiments, Table 1 shows the specification of the CGR18650CH LiB obtained from the manufacturer.

BaSyTec 32 channels Cell Test System (CTS) and BaSyTest Battery-Test-Software Version 5.6.1.20 are used for the experiments. The battery characteristics shown in Table 1 are added and stored in the BaSyTec's database, so that each battery under test can have its individual signature in the database. In order to obtain a good connection with lower contact resistance, spot welding machine is used to connect the battery cell to CTS.

A general set-up in the Test Control Software for all experiments in this work is programmed as follows:

- All fresh battery cells are firstly discharged to the cut-off voltage of 3 V as specified in the battery specification.
- The charging process is carried out at a fixed charging rate of 0.7C in CC mode and a voltage of 4.2 V in CV mode with a charge-termination current of 110 mA, according to the company specification shown in Table 1. Since this work focus only on the discharging process, the charging condition is fixed for all cases.
- The terminal voltage and current of the cell are continuously monitored and recorded every 20 s to obtain sufficient number of data points used in the fitting process.
- In order to provide fast SoC estimation, 10 min is chosen as battery rest time after charging before the discharging experiments. The typical long rest periods reported in the literature are not chosen since it is not suitable in practical applications such as EV [27]. In order to justify the use of such short rest time, the effect of rest time on the accuracy of SoC estimation will be discussed in the later part of this Section.
- All the experiments are performed under Lab's constant ambient temperature of 23 °C

Model verification and the determination of n using constant discharging current are to be carried out first. Specific time varying current will then be used once our model parameters and n values are determined.

3.1. Constant discharging current

The experimental discharge curve of Panasonic's CGR18650CH LiB with constant discharging current of 2C is shown in Fig. 7. Table 2 lists out the best fitted parameters values for different n, and Fig. 8 shows the variation of the key parameters values vs. n. Here $m_1 = 1$ and $m_2 = 0.5$ as expected from a fresh battery.

To simplify the fitting, the emf expression in Eq. (12) is re-written as follows.

Table 2
Estimation of battery discharging model's parameters for different number of RC groups.

n	R_1 (Ω)	R_1C_W (s)	$R_e + R_{CT}$ (Ω)	Q_m (Ah)	m_1	m_2	k (Ω)	α	β	rmse (V)
1	0.643	2298	0.0315	2.1812	1.0	0.5	0.0028	3.955	1.0989	0.0045
2	1.212	8915	0.0526	2.1480	1.0	0.5	0.0016	4.047	0.9737	0.0053
3	0.960	13075	0.0520	2.1216	1.0	0.5	0.0009	4.043	0.5155	0.0064
4	0.989	19211	0.0458	2.1102	1.0	0.5	0.0006	4.014	0.3761	0.0069
5	0.407	10837	0.0489	2.0716	1.0	0.5	0.0000	4.029	0.0001	0.0106
6	0.414	11606	0.0465	2.0848	1.0	0.5	0.0002	4.026	0.0002	0.0110
7	0.154	1653	0.0436	2.1060	1.0	0.5	0.0005	4.057	0.0000	0.0134
8	0.148	1518	0.0435	2.1127	1.0	0.5	0.0006	4.062	0.0000	0.0136
9	0.146	1473	0.0432	2.1157	1.0	0.5	0.0007	4.062	0.0000	0.0137
10	0.144	1445	0.0426	2.1178	1.0	0.5	0.0007	4.062	0.0000	0.0139
11	0.143	1426	0.0424	2.1194	1.0	0.5	0.0007	4.063	0.0000	0.0140
12	0.142	1409	0.0425	2.1209	1.0	0.5	0.0008	4.064	0.0000	0.0140
13	0.142	1400	0.0423	2.1217	1.0	0.5	0.0008	4.064	0.0000	0.0141
14	0.141	1387	0.0422	2.1229	1.0	0.5	0.0008	4.065	0.0000	0.0142
15	0.141	1380	0.0420	2.1236	1.0	0.5	0.0008	4.065	0.0000	0.0142
16	0.141	1376	0.0418	2.1242	1.0	0.5	0.0008	4.065	0.0000	0.0143
17	0.140	1369	0.0417	2.1249	1.0	0.5	0.0008	4.065	0.0000	0.0143
18	0.140	1369	0.0417	2.1249	1.0	0.5	0.0008	4.065	0.0000	0.0143

$$V_{\text{emf}} = \alpha + \beta - \frac{RT}{F}\left\{\ln\frac{[2-(2-m_1)\text{SoC}][2m_2-(2-m_1)\text{SoC}]}{[2m_1-2+(2-m_1)\text{SoC}][(2-m_1)\text{SoC}]}\right\} \quad (20)$$

where $\alpha = E_0 - RT/F\left[U^+/m_1 + \varepsilon\right]$, and $\beta = RT/F\left[2 - m_1/2m_1m_2 \times \text{SoC} \times (m_2U^+ - m_1U^1)\right]$

From Fig. 8 and Table 2, it can be seen that when n is small, the parameters values fluctuate, and they converge when n is greater than 15. Although $n = 3$ is the commonly used in many literature, the experimental results show that it is insufficient to ensure good accuracy in the estimation. In fact, the computation time for the RC group of $n = 15$ is only 0.3 s which is insignificantly small. The final n and model parameters' values for the LiB studied are listed in Table 3, and it can also be seen that the fitting accuracy is very good from Table 3 and Fig. 7.

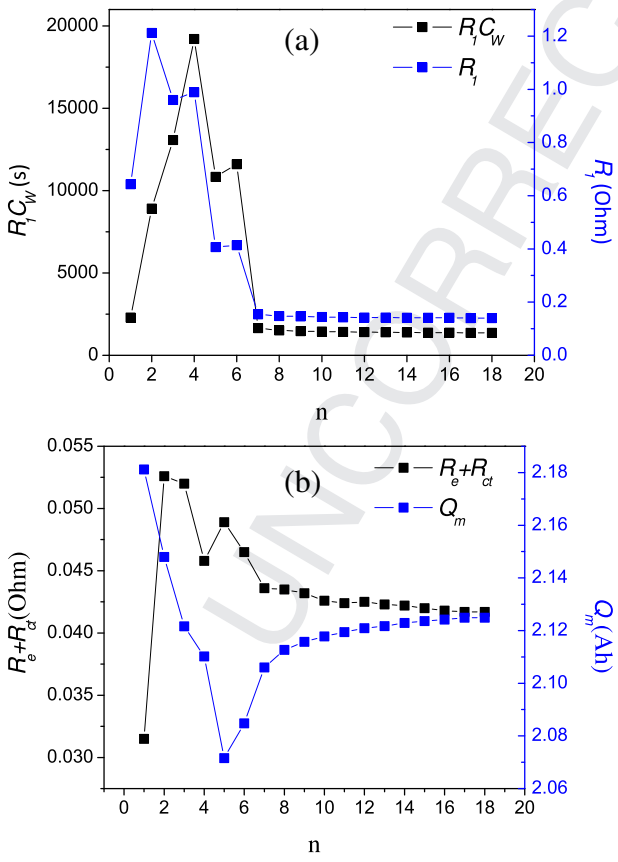

Fig. 8. (a). Variation of R_1 and R_1C_W with different value of n. (b). Variation of $R_e + R_{CT}$ and Q_m with different value of n.

Therefore, given a discharge curve of a LiB cell, the Q_m can be determined after each discharge cycle without the need to fully discharge the cell.

Since the proposed model is derived based on the electrochemistry processes in the battery discharging process, the proposed model is expected to provide the same experimental EIS spectrum with the parameters determined from the discharge curve. This also serves to further verify the accuracy of the proposed model.

C_{DL} and R_e are firstly estimated from the experimental EIS spectrum by using the equivalent circuit in Fig. 3, and then together with the model parameters from Table 3, the Nyquist plot of the LiB cell at various frequencies with the battery terminal voltage at 4.0 V (with a corresponding SoC) is computed. The comparison of the computed and experimental EIS spectrums is shown in Fig. 9, and one can see a good agreement in the comparison.

3.2. Rest time experiments

In order to obtain stable terminal voltage of LiB, a rest period of at least 12 h after the battery is fully charged is specified, i.e. the battery can start to discharge only after the rest period. The purpose of the rest period is to regain the chemical equilibrium at the electrodes and compensates for the self-discharge after charging [28]. In order to mimic practical application, the experiments performed in this work are done, however, with the rest time of only 10 min as mentioned earlier. In order to examine the impact of such short rest time, the following rest time experiments are conducted.

A cell is discharged at 2C-rates with different rest time (10 min, 30 min, 1 h, 6 h and 12 h) after it is fully charged. The respective discharging curves at different rest time conditions are used to estimate the model parameters, and the results are shown in Table 4

The battery is in a state of non-equilibrium when current flows in and out during charging and discharging. This non-equilibrium causes the average concentration of the reacting species in the bulk and at the electrode surface to be different. A mass transport effect is mainly responsible for this difference, and diffusion is

Table 3
Estimation of battery discharging model's parameters using 15 of RC groups for the Warburg elements.

n	R_1 (Ω)	R_1C_W (s)	$R_e + R_{CT}$ (Ω)	Q_m (Ah)	m_1	m_2	k (Ω)	α	β	rmse (V)	Accuracy
15	0.141	1380	0.042	2.1236	1.0	0.5	0.0008	4.065	0	0.0142	0.9964

commonly treated as main contributor for the mass transport effect [18,29]. This diffusion results in locally changed ion concentration at the location of charge transfer reaction, therefore the reaction rate at the electrode is influenced by mass transport process [13,18]. With longer rest period, the ion concentration at the electrodes decreases and distributes more uniformly into the electrolyte, and hence this implies a smaller Warburg coefficient. This is indeed observed in Table 4 where a decrease in the values of R_1 and R_1C_W can be seen. Also, due to the increased concentration of cation at the cathode side after charging, the cell's capacity appears to be higher. As the cell rests, the capacity decreases to its stable value. In other word, the proposed model does reflect the non-equilibrium process in the battery cell in consistent with the electrochemistry.

From Table 4, it can therefore be seen that the values of the model parameters are indeed influenced by the length of rest period, but the impact is insignificant. For example, the different in Q_m estimation is less than 0.5%, and thus the inaccuracy of SoC estimation resulted from short rest period is very small. To speed up the experimentation, 10 min rest period is employed in all the experiments in this work.

3.3. Effect of discharging current

The previous experiments are performed at a constant discharging current of 2C. In most practical applications, the discharging current varies during operation, and additional experiments are therefore conducted with discharging current of 1C, 1.5C and 2C to examine the impact of the discharging current on the model parameters. The results are shown in Table 5.

Larger discharging current forces the diffusion of the ionic species to move faster in the electrolyte, and thus the measured Warburg element will be smaller as seen in Table 5. With larger discharging current, it is proposed that the charge stored in the negative electrode, Q_z^- in Eq. (7) will also be smaller as too many charges arriving at the negative electrode per unit time will render inefficient storage of charges. Therefore, z_{Li} in Eq. (8) will be smaller,

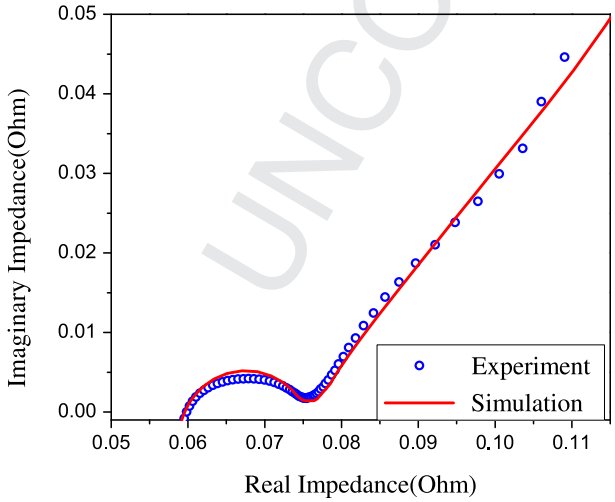

Fig. 9. Comparison of Experimental and computed EIS spectrum of Panasonic's CGR18650CH LiB cell at 4 V OCV.

and thus for a given m_1, the apparent SoC will be smaller. But the total charge delivered as obtained from Coulomb counting method is fixed, and based on the SoC formulae, the apparent Q_m will be smaller with large discharging current as observed in Table 5.

Since discharging current affect the model parameters, the values in Table 5 are used to determine the discharge curve of the LiB cell with step change in the discharging current, with 30 min in between the step change. Comparison of the computation and experimental results are shown in Fig. 10 and the maximum error in the battery voltage is 0.0808V with the root mean square error of only 0.0326 V, which is very small. The larger deviation occur at lower battery voltage (or correspondingly lower SoC) is due possibly to the fact that the proposed model is developed with SoC limited to above 50% (Fig. 11).

With the results shown in Fig. 10, it can been seen that the proposed model can be extended to varying discharging current if the discharging current is discretized. As the model parameters are affected by the discharging current as shown in Table 5, one has to obtain the relationship of these parameters values with the discharging current levels. Experimental verification are being performed and the results will be reported in future as this work focus only the framework developed for in-situ online battery parameters estimation.

As mentioned earlier, the main problem with the Coulomb counting method is the knowledge of Q_m. Using the model developed in this work, one can determine the Q_m easily after every discharge cycle, and hence the estimation of SoC using Coulomb counting method can be accurate with the above flow-chart. The method is fast and accurate, taking approximately 0.3011 s, and can easily be implemented in most practical applications.

4. Conclusion

Maximum charge capacity of a battery at the beginning of each discharge cycle is an important parameter for accurate estimation of SoC using Coulomb counting method. Its value can also be used as an indication of state-of-health (SoH) of a battery. In this work, a

Table 4
Estimation of battery discharging model's parameters at different rest time condition.

Rest time	R_1 (Ω)	R_1C_W (s)	$R_e + R_{CT}$ (Ω)	Q_m (Ah)	m_1	m_2	rmse (V)	Accuracy
10 min	0.323	8252	0.0012	2.19	1.0	0.5	0.0120	0.9973
30 min	0.315	8259	0.0013	2.18	1.0	0.5	0.0122	0.9972
1 h	0.315	8165	0.0011	2.17	1.0	0.5	0.0129	0.9969
6 h	0.315	8187	0.0014	2.17	1.0	0.5	0.0116	0.9960
12 h	0.315	8184	0.0016	2.17	1.0	0.5	0.0114	0.9966

Table 5
Model Parameters determined from discharging curves at different discharging currents.

Discharging current	R_1 (Ω)	R_1C_W (s)	R_e+R_{CT} (Ω)	Q_m (Ah)	m_1	m_2	rmse (V)	Accuracy
2C	0.140	1360.65	0.000874	2.13	1	0.5	0.0144	0.996
1.5C	0.159	1533.19	0.000108	2.18	1	0.5	0.0148	0.996
1C	0.175	2045.91	0.000176	2.17	1	0.5	0.0153	0.996

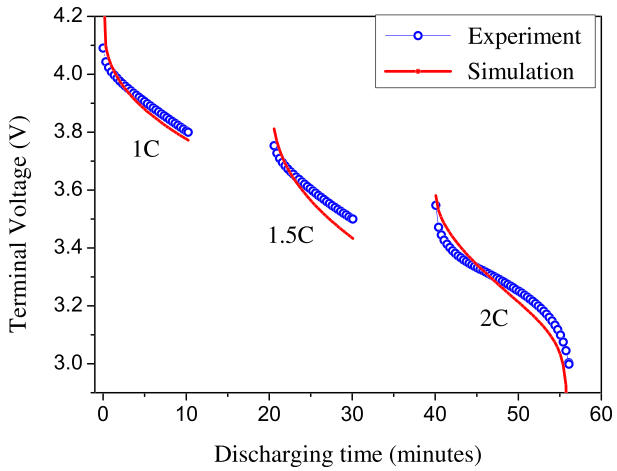

Fig. 10. Comparison of our computed and experimental discharge curve for varying discharging current.

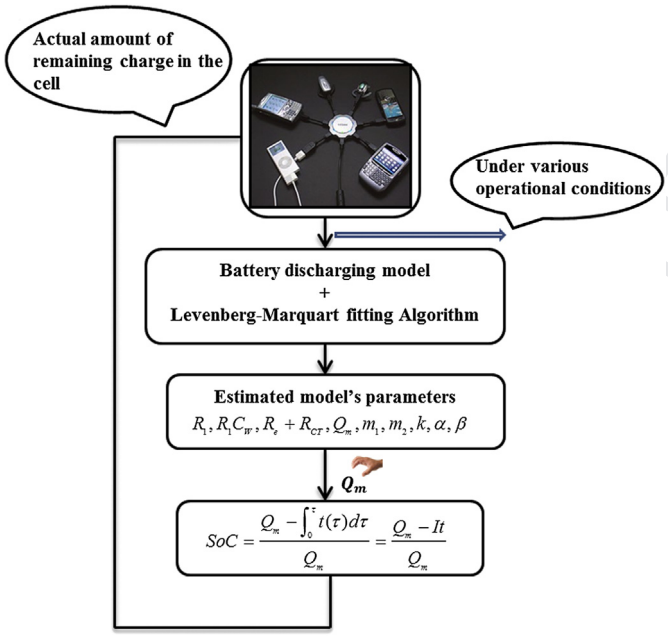

Fig. 11. An implementation flow-chart of SoC estimation.

practical electrical framework is developed for in-situ online battery parameters estimation, based on the electrochemistry principle in the battery during discharging. This model is in contrast to many other electrical models where are derived by intelligent electronic components selection and connection so as to resemble the particular experimental discharge curve but without the connection to its electrochemistry processes. The latter suffers from its lack of generality while the model developed is applicable to all LiB cells. The model developed is able to provide the maximum charge capacity online after each discharge cycle without the need to fully discharge a cell which can shorten the lifespan of a cell.

Experimental verification of the model developed shows good agreement, both in temporal as well as frequency space in the form of EIS spectrum. Its application to time varying current during discharging is also shown through step current change with slightly different model parameters as they are affected by the discharging currents. Application to actual time varying current is possible through a database or calibration curves of the model parameters values at different discharging currents.

The model developed allows the internal parameters of a cell to be determined which can be useful to determine the degraded components in the cell when the cell is aged or damaged [30]. It can also be a useful tool to evaluate the quality of LiB cells non-destructively.

Acknowledgements

The authors wish to thank TUM CREATE program is a joint research programme between Technische Universität München (TUM) in Germany and Nanyang Technological University (NTU) in Singapore with funding by the National Research Foundation of Singapore for providing the equipment for testing.

References

[1] M. Armand, J.M. Tarascon, Nature 451 (2008) 652–657.
[2] V. Pop, H.J. Bergveld, D. Danilov, P.H.L. Notten, P.P.L. Regtien, Battery Management Systems: Accurate State-of-charge Indication for Battery-powered Applications, Springer Science, B.V, 2008.
[3] S. Piller, M. Perrin, A. Jossen, in: 22nd IPSS, Elsevier, Switzerland, 2001, pp. 113–120.
[4] M. Coleman, L. Chi Kwan, Z. Chunbo, W.G. Hurley, IEEE Trans. Ind. Electron. 54 (2007) 2550–2557.
[5] N. Kong-Soon, H. Yao-Feng, M. Chin-Sien, H. Yao-Ching, in: Intelec, 31st International, 2009, pp. 1–5.
[6] I. Snihir, W. Rey, E. Verbitskiy, A. Belfadhel-Ayeb, P.H.L. Notten, J.Power Sources 159 (2006) 1484–1487.
[7] G.L. Plett, J.Power Sources 134 (2004) 252–261.
[8] G.L. Plett, J.Power Sources 134 (2004) 262–276.
[9] G.L. Plett, J.Power Sources 134 (2004) 277–292.
[10] G.L. Plett, J.Power Sources 161 (2006) 1356–1368.
[11] G.L. Plett, J.Power Sources 161 (2006) 1369–1384.
[12] Serge pelissier, in: VPPC, IEEE, Lille, FR, 2010.
[13] A.J. Bard, L.R. Faulkner, Electrochemical Methods: Fundamentals and Applications, Wiley, 2000.
[14] R. Yazami, in US Patent #611726459, 2012.
[15] V. Pop, H.J. Bergveld, P.P.L. Regtien, J.H.G. Op Het Veld, D. Danilov, P.H.L. Notten, J. Electrochem. Soc. 154 (2007) A744–A750.
[16] R.C. Kroeze, P.T. Krein, in: PESC 2008, IEEE, 2008, pp. 1336–1342.
[17] C. Min, G.A. Rincon-Mora, IEEE Trans. Energy Convers. 21 (2006) 504–511.
[18] J.E.B. Randles, Discuss. Faraday Soc. 1 (1947) 11–19.
[19] A. Jossen, J.Power Sources 154 (2006) 530–538.
[20] D. Andre, M. Meiler, K. Steiner, H. Walz, T. Soczka-Guth, D.U. Sauer, J.Power Sources 196 (2011) 5349–5356.
[21] V. Pop, H.J. Bergveld, J.H.G.O. Veld, P.P.L. Regtien, D. Danilov, P.H.L. Notten, J. Electrochem. Soc. 153 (2006) 2013–2022.
[22] C.M. Shepherd, J. Electrochem. Soc. 112 (1965) 657–664.
[23] E. Kuhn, C. Forgez, G. Friedrich, in: EVS 20, Long Beach, CA, 2003.
[24] C.M. Tan, Simulated Annealing, In Tech, 2008.
[25] J. Stalnaker, E. Miller, in: Geoscience and Remote Sensing Symposium, 2007. IGARSS 2007, IEEE International, 2007, pp. 432–435.
[26] CGR18650CH Lithium Ion, Panasonic Corporation of America, 2011. Available from: http://www.panasonic.com/industrial/includes/pdf/cgr18650ch_%20datasheet.pdf.
[27] W.X. Shen, C.C. Chan, E.W.C. Lo, K.T. Chau, IEEE Trans. Ind. Electron. 49 (2002) 677–684.
[28] I. Buchmann, Batteries in a Portable World, Cadex Electronics, Richmond, 2001.
[29] H.J. Bergveld, W.S. Kruijt, P.H.L. Notten, Battery Management Systems: Design by Modelling, Springer, Netherlands, 2002.
[30] F. Leng, C.M. Tan, A. Raghavendra, A. Jossen, in: 4th International Conference Battery Safety, Knowledge Foundation, San Diego, CA USA, 2013.